

Numerical Simulation of Similar and Dissimilar Materials Welding Process; Quantifications of Temperature, Stress, Strain and Deformation

Ranjit Shrestha¹, Wontae Kim^{1, †}, Heesang Park² and Jeonghak Park³

¹Division of Mechanical & Automotive Engineering, Kongju National University, Cheonan, Korea
sthranjit@gmail.com

Corresponding Author E-mail: kwt@kongju.ac.kr

²Technology development team, Korea Research Institute of Smart Material and Structures System Association, Daejeon, Korea
m55nring@naver.com

³Safety measurement Center, Korea Research Institute of Standards and Science, Daejeon, Korea
parkjh@kriss.re.kr

Abstract - In the present paper, 3 Dimensional welding simulation was carried out in the FE software ANSYS in order to predict temperature, stress, strain and deformation in the joining of similar and dissimilar materials. The numerical simulation shows that temperature exceeds well above the melting temperature of the substrate material in the welding region. It is found that, higher residual stress is distributed in the weld bead area and surrounding heat affected zone. The stress and strain distribution patterns in the specimen showed that both tended to concentrate at or near points of application of thermal load, and were generally not uniform in these areas. It is also found that Stress and strain were concentrated at corners, edges, and other areas of abrupt change in the shape of the specimen and was also not uniform where the cross-section of the structure changed suddenly, and had large gradients at localized points. The deformation was found maximum at the beginning and the end of welding direction (Y-axis) and minimum at the ends of X-axis as they are simply supported in both ends. In addition, among the six different cases of similar and dissimilar materials (S40C+S40C, STS304+STS304, STS316L+STS316L, S40C+STS304, S40C+STS316L, STS304+STS316L), the minimum temperature was found in S40C+STS304 whereas the maximum temperature was S40C+STS316L; the minimum stress was found in case of S40C+STS304 and maximum stress was found in S40C+STS316L; the minimum strain was found in case of S40C+STS304 and maximum strain was found in STS304+STS304; the minimum deformation was found in S40C+S40C and maximum in S40C+STS316L. The prediction show qualitative good agreement with the experimental results found in the literature and hence it was confirmed that the method of finite elements has proved to be successful for proper design analysis.

Keywords: Finite Element Analysis, ANSYS, temperature, stress, strain, deformation.

I. INTRODUCTION

Welding is a reliable and efficient metal joining process. Many metallic structures in industry are assembled through some kind of welding process which is composed of heating, melting and solidification using a heat source such as arc, laser, torch or electron beam. The highly localized transient heat and strongly nonlinear temperature fields in both heating and cooling processes cause non-uniform thermal expansion and contraction, and thus result in plastic deformation in the weld and surrounding areas. As a result, residual stress, strain and distortion are permanently produced in the welded structures. High tensile residual stresses are known to promote fracture and fatigue, while compressive residual stresses may induce undesired, and often unpredictable, global or local buckling during or after the welding. These adversely affect the fabrication, assembly, and service life of the structures. Therefore, prediction and control of residual stresses and distortion from the welding process are extremely important in industry. In order to better understand the welding process and its effects on structures, engineers and researchers around the world, covering a large number of industries, have been trying to create algorithms and methodologies to simulate the complete process or just individual phases. The distribution of welding residual stress depends on several main factors such as structural dimensions, material properties, restraint conditions, heat input, number of weld pass and welding sequence. In many high temperature applications, it is necessary to join together components of same or different chemical, physical and mechanical properties. Undoubtedly, the joining of dissimilar metals is more challenging due to differences in the properties of the base metal welded [1-4].

Over the past 20 years, research has been conducted enabling the use of advanced analytical procedures to more accurately simulate the welding process. Due to the complexity of the physical processes involved in welding, however, simple mathematical solutions cannot address the practical manufacturing processes. Furthermore, it is also impossible for any experimental technique to obtain a complete mapping of the residual stress and distortion distribution in a general welded structure. Numerical simulation thus plays an indispensable role in the integrity analysis of such welded structure. In principle, a finite element simulation of the welding process consists of two main parts: thermal analysis and mechanical stress analysis. In thermal analysis, the temperature field is determined as a function of time for each integration point. This temperature time-history is used as an input into the thermal stress analysis. Herein, the thermal solution can be sequentially or fully coupled with the mechanical solution of the structure. Because the rate of heat generation due to mechanical dissipation energy can be neglected in the heat transfer analysis, a sequentially coupled thermal-stress analysis is commonly applied for the simulation of a welding process in which a thermal analysis is followed by a stress analysis [5-12]

II. NUMERICAL FEM APPROACH

A. Theory

To simulate the gas metal arc welding (GMAW), 3D simulation model has been developed by using a commercial finite element modeling computer package 'ANSYS Version 14.0'. In the thermal analysis, the finite element formulation is based on the governing equation for transient nonlinear heat transfer analysis in the form,

$$\frac{\partial}{\partial x} \left(k_x \frac{\partial T}{\partial x} \right) + \frac{\partial}{\partial y} \left(k_y \frac{\partial T}{\partial y} \right) + \frac{\partial}{\partial z} \left(k_z \frac{\partial T}{\partial z} \right) + Q = \rho C \frac{\partial T}{\partial t} \quad (1)$$

where, k_x , k_y , and k_z are the thermal conductivities in the x, y and z directions respectively, T is the temperature, Q is the heat generation, ρ is the density, C is the specific heat capacity and t is the time. A general solution of Eq. (1) is obtained by introducing the following initial and boundary conditions:

$$T(x, y, z, t = 0) = T_0(x, y, z) \quad (2)$$

$$\left(k_x \frac{\partial T}{\partial x} N_x + k_y \frac{\partial T}{\partial y} N_y + k_z \frac{\partial T}{\partial z} N_z \right) + q_s + h_c(T - T_\infty) + h_r(T - T_r) = 0 \quad (3)$$

where N_x , N_y , and N_z are the direction cosine of the normal to the boundary, h_c and h_r are the convection and radiation heat transfer coefficients respectively, q_s is the boundary heat flux, T_r denotes the temperature of radiation and T_∞ represents the surrounding temperature. Radiation heat losses are dominant near the weld and can be expressed by the following equation

$$h_r = \sigma \epsilon F (T^2 + T_r^2)(T + T_r) \quad (4)$$

where, $r = 5.67E-7 \text{ J/(m}^2 \text{ K}^4)$ is the Stefan-Boltzmann constant, ϵ is the effective emissivity and F is the configuration factor. The numerical simulation of the welding process is performed by applying a distributed heat flux to the weld elements. In so doing, the total heat input is given by:

$$Q = \eta_A * \left(\frac{V * I}{1000 * W_s} \right) \quad (5)$$

where, η_A is welding efficiency, V is welding arc voltage, I is welding current; V is welding arc voltage; W_s is the arc welding speed, and Q is the heat input.

The heat input from weld electrode is modeled by using heat flux as input from electrode to weld surface and is depends on the efficiency of arc and welder setting.

$$q = \frac{Q}{a} \quad (6)$$

where, q =heat flux and a is the area of electrode [3-5].

The corresponding finite element equations of thermal and mechanical are obtained by choosing a form of interpolation function representing the variation of the field variables, namely temperature, T and displacement, U, within the corresponding finite elements of the structural model and by applying further the weighted-residual or vibrational argument to the mathematical models.

$$[C]\{T\} + [K]\{T\} = \{FT\} \quad (7)$$

in which,

$$[C] = \int_V \rho C [N]^T [N] dV \quad (8)$$

$$[K] = \int_V k [B]^T [B] dV + \int_S h_f [N]^T [N] dS \quad (9)$$

$$[F_T] = \int_V Q [N]^T dV + \int_S h_f T_{ref} [N]^T dS \quad (10)$$

where, ρ is the density (kg/m^3), c is the specific heat (J/kg. K), k is the conductivity (W/m. K), h_f is the convective heat transfer coefficient ($\text{W/m}^2 \text{. K}$), Q is the rate of internal heat generation per unit volume (W/m^3), [N] is the

matrix of element shape functions, [B] is the matrix of shape functions derivative, and {T} is the vector of nodal temperature.

The results of temperature distribution and history obtained from Eq. (7) are then inserted into the mechanical model in the form of thermal load. Incorporating the elasto-plasticity analysis, the mechanical finite element equation may be written in the form of incremental as:

$${}^{i+1}[K_1] \{\Delta U\} - {}^{i+1}[K_2] \{\Delta T\} = {}^{i+1}\{R\} - {}^i\{R\} \quad (11)$$

in which,

$$[K_1] = \int_V [B]^T [D^{ep}] + [B] dV \quad (12)$$

$$[K_2] = \int_V [B]^T [C^{th}] + [M] dV \quad (13)$$

$$\{R\} = \int_S [N]^T \{p\} dS + \int_V [N]^T \{f\} dV \quad (14)$$

$$[D^{ep}] = [D^e] + [D^p] \quad (15)$$

where, {ΔU} is the incremental of nodal displacement, {ΔT} is the incremental of nodal temperature, [B] is the matrix of strain-displacement, [D_e] is the matrix of elastic stiffness, [D_p] is the matrix of plastic stiffness, [C_{th}] is the matrix of thermal stiffness, [M] is the temperature shape function, {p} is the vector of traction or surface force, {f} is the vector of body force, and i is the current step of analysis.

The vector of nodal displacement at the next step of analysis, i+1{U} could be obtained from:

$${}^{i+1}\{\sigma\} = {}^i\{\sigma\} + \{\Delta\sigma\} \quad (16)$$

$$\{\Delta\sigma\} = [D^{ep}][B]\{\Delta U\} + [C^{th}][M]\{\Delta T\} \quad (17)$$

Commonly, the iterative method of Newton-Raphson is employed in the finite element solver to solve the nonlinear equations. From the thermal analysis results, the updated stress and displacement conditions are now obtained [6].

B. Materials and methods

The gas metal arc welding (GMAW) is modeled in the present welding simulation. Fig. 1 and 2 shows the welding configuration and geometry of the specimen under consideration. As shown in the figure, the moving torch is applied on the longitudinal upper edge of the plate of 200 mm long, 70 mm wide and 1.45 mm thick. The plate is simply supported at both ends.

In this study, materials used for the welding simulation were S40C, STS 304 and STS316L with the material properties vary according to the temperature history and six cases as shown in Table I (S40C+S40C, STS304+STS304, STS316L+STS316L, S40C+STS304, S40C+STS316L, STS304+STS316L) for welding of similar and dissimilar metals were considered. Each case contains two parts, A material and B material. A material and B material are same for the case of similar material welding process and different for the cases of dissimilar material welding process.

A thermal analysis of heat conduction was carried out in the first step to obtain temperature distribution histories over the structural model. In the thermal analysis, the welding heat input, Q was calculated and the arc efficiency, η_A for GMAW was assumed to be 0.80. Also, the values of convective heat transfer coefficient, h_f was taken as stagnant air-simplified case and reference temperature was taken 22°C. The Table I shows the welding parameters for different six cases used in this analysis whereas the Table II show the thermal and mechanical properties of the materials. In the next step, a structural analysis was carried out to obtain the mechanical response of the structural model, where the temperature history obtained from the first step was employed as a thermal load in the analysis. The material model of elasto-plastic based on the Von Mises yield criterion and isotropic strain hardening rule was chosen, in which its response over the history was determined by the temperature-dependent material properties inputted. The boundary condition or constraint on the structural model needs also to be assigned accordingly.

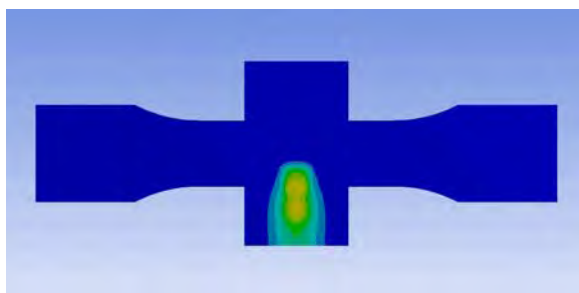


Fig.1. Configuration of the welding specimen.

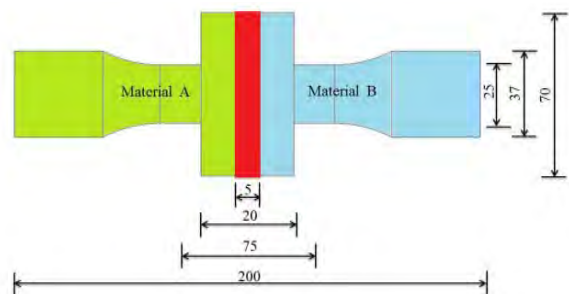


Fig.2. Geometry of the welding specimen.

TABLE I Welding Parameters for different cases

Cases	Material A	Material B	Speed (mm/s)	Current (A)	Voltage (V)	Heat Flux (W/mm ²)
1	S40C	S40C	10	20.1	115.6	0.5311
2	STS 304	STS 304	10	18.4	120.0	0.5047
3	STS316L	STS316L	10	18.3	117.6	0.4919
4	S40C	STS 304	10	18.9	126.1	0.5448
5	S40C	STS316L	10	19.6	125.4	0.5618
6	STS304	STS316L	10	18.4	118.7	0.4992

TABLE II Thermal and mechanical properties of the materials

Properties	Materials		
	S40C	STS304	STS316L
Density(kg/m ³)	7753	7900	8000
Specific Heat (J/kg-K)	486	477	500
Thermal Conductivity(w/m ⁰ C)	36	16.2 @ 100 ⁰ C 21.5 @ 500 ⁰ C	16.3 @ 100 ⁰ C 21.4 @ 500 ⁰ C
Young Modulus(Gpa)	191.69	161.86	179.14
Poisson's ratio	0.315	0.384	0.349
Coefficient of thermal expansion (µm/m/°C)	1.1E-6 @ 100 ⁰ C	1.72E-6 @ -100 ⁰ C 1.78E-6 @ 315 ⁰ C	1.59E-6 @ -100 ⁰ C 1.62E-6 @ 315 ⁰ C

III. FEM RESULTS

At first, setup of a thermal analysis was done to determine thermal state in the weld and surrounding components. Following this thermal loading was import to setup structural analysis which results in deformation, residual stress & strain.

The fig.4 shows the simulation results of temperature, stress, strain and deformation profile in the joining of similar materials for the case of (S40C+S40C). The result shows that temperature exceeds well above the melting temperature of the substrate material in the welding region. It is found that the higher residual stress is distributed in the weld bead area and surrounding heat affected zone. Both the stress and strain distribution patterns in the specimen showed that both tended to concentrate at or near points of application of thermal load, and stress & strain fields were generally not uniform in these areas. Stress & strain were concentrated at corners, edges, and other areas of abrupt change in the shape of the specimen and was not uniform where the cross-section of the structure changed suddenly, and had large gradients at localized points. The deformation was found maximum at the beginning and the end of welding direction (Y-axis) and minimum at the ends of X-axis as they are simply supported in both ends.

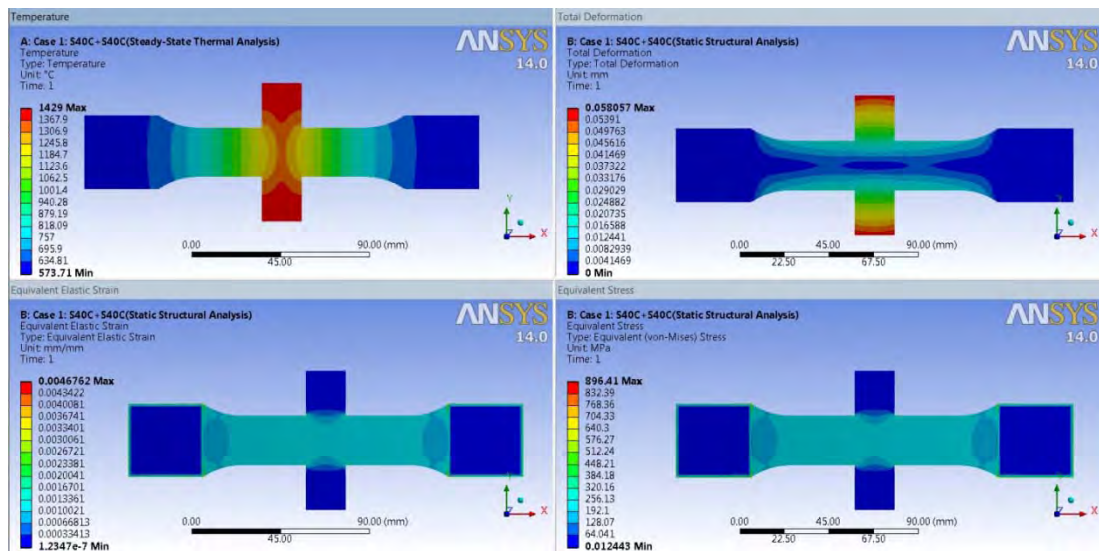


Fig.4.Simulation results of temperature, stress, strain and deformation of similar materials (S40C+S40C)

For the measurement of temperature, deformation, strain and stress distribution pattern at different location, measurement profile 1-2 (90, 0, 0) & (110, 0, 0) was created in X-axis (as shown in fig. 5). The fig. 6 shows the measurement of temperature, deformation, strain and stress distribution pattern along the profile 1-2 for the similar welding materials of case S40C+S40C. Since both the materials A and B are same, the temperature, stress, strain and deformation distribution profile seems symmetric about Y axis, from the center line of the specimen.

Following the same procedure, the measurement of temperature, deformation, strain and stress distribution pattern along the measurement profile 1-2 (90, 0, 0) & (110, 0, 0) was plotted for the case of STS304+STS304, STS316L+STS316L, S40C+STS304, S40C+STS316L, STS304+STS316L (as shown in fig. 7,8,9,10 and 11).

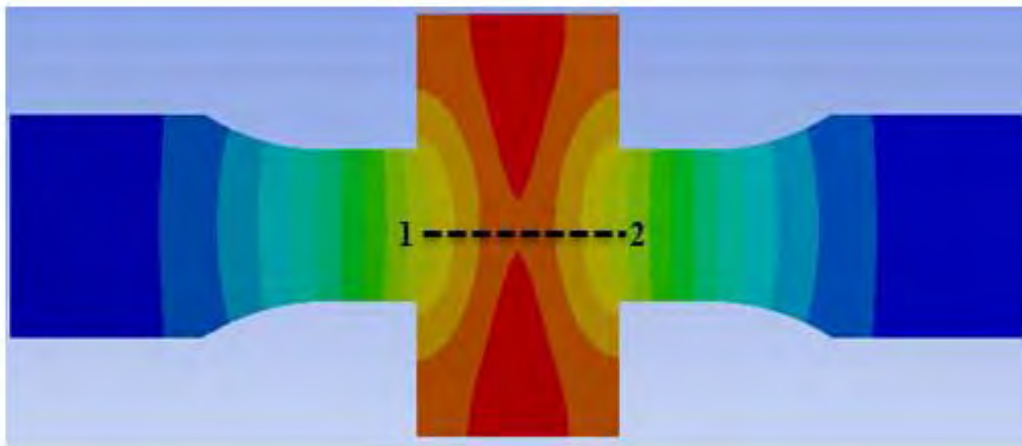


Fig. 5: Measurement profile 1-2 at [(90, 0, 0) & (110, 0, 0)]

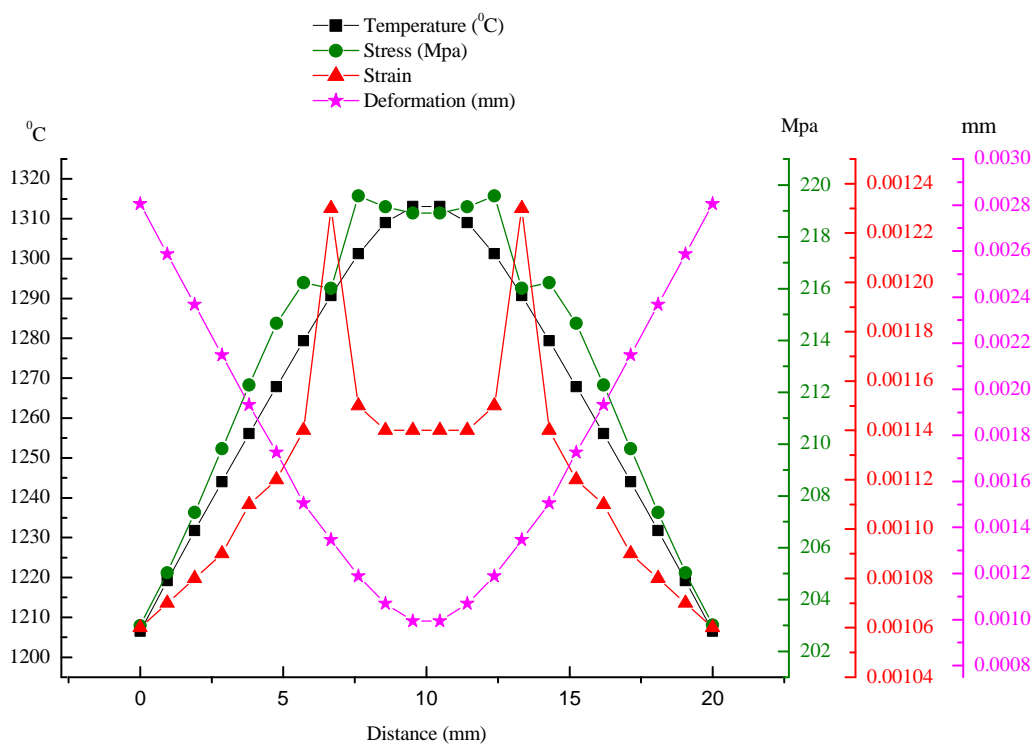
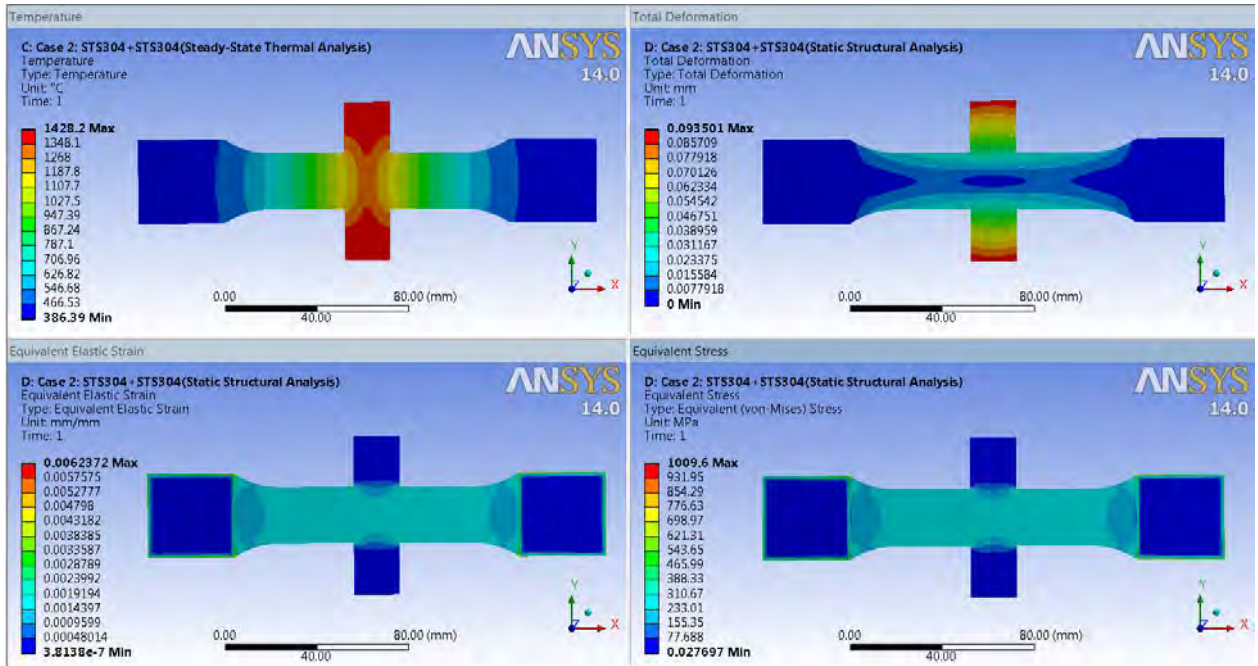
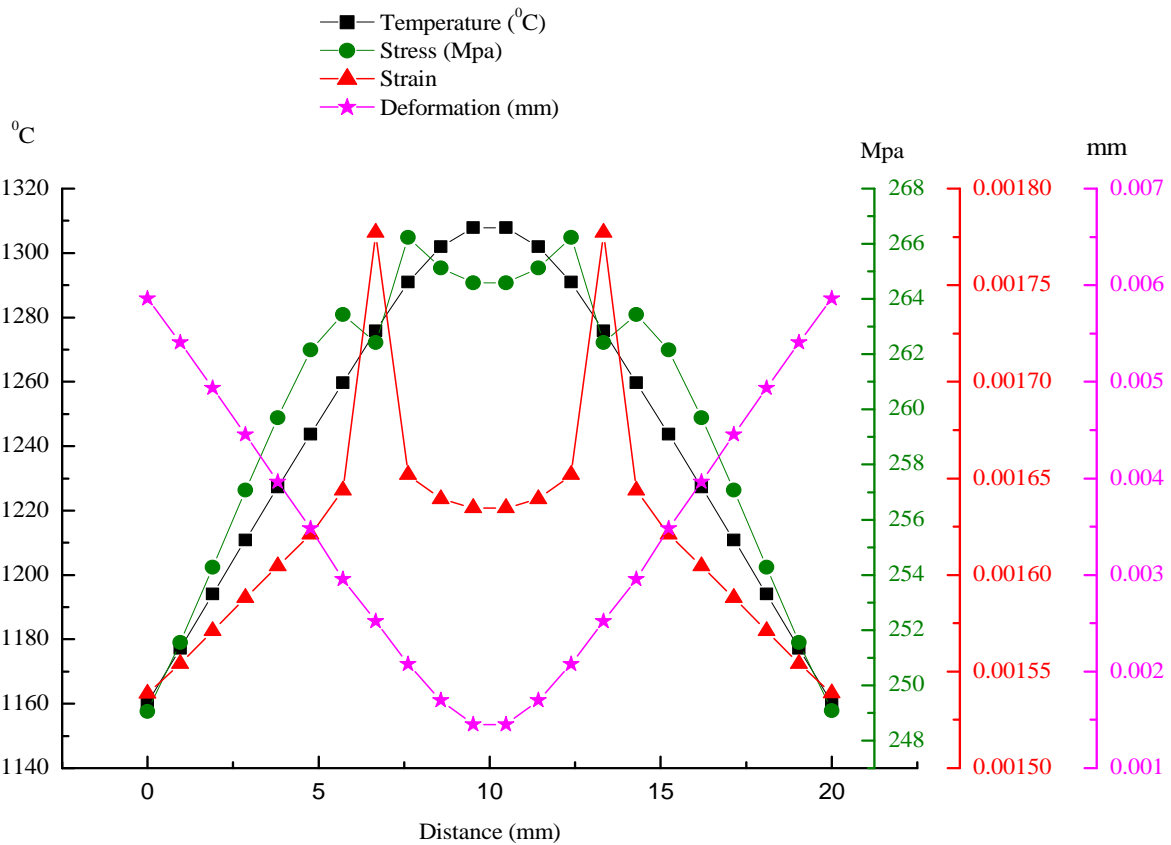


Fig.6. Temperature, stress, strain and deformation at profile 1-2 (S40C+STS304)

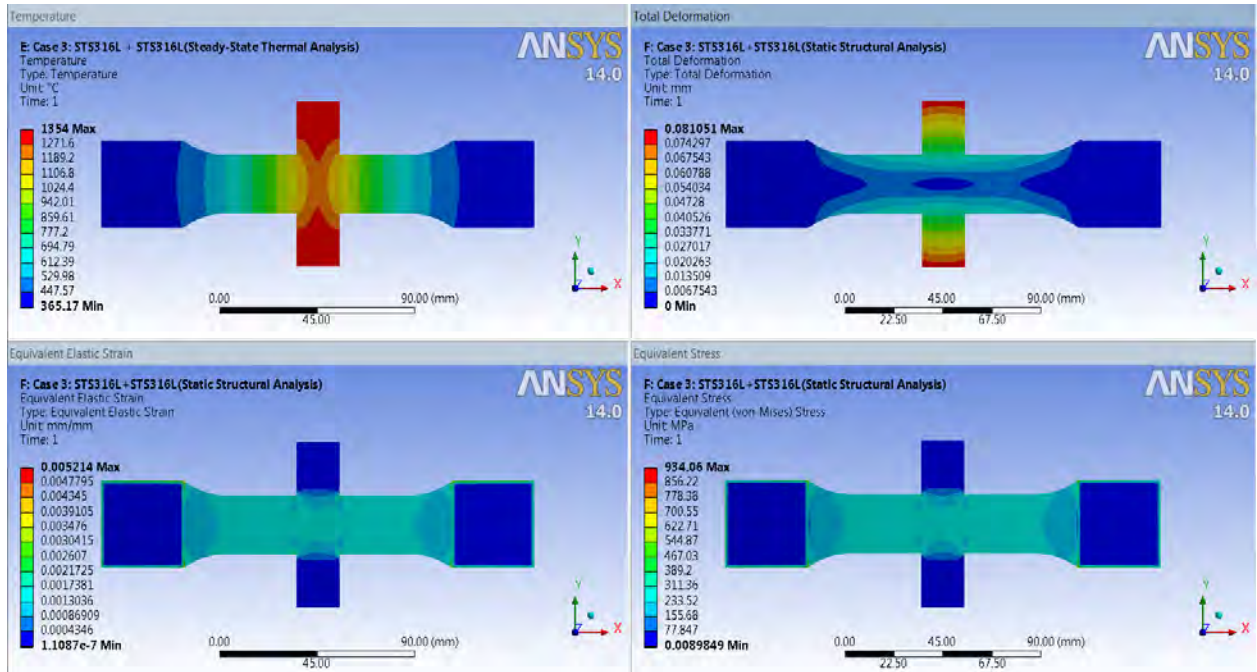


a) Simulation results of temperature, stress, strain and deformation

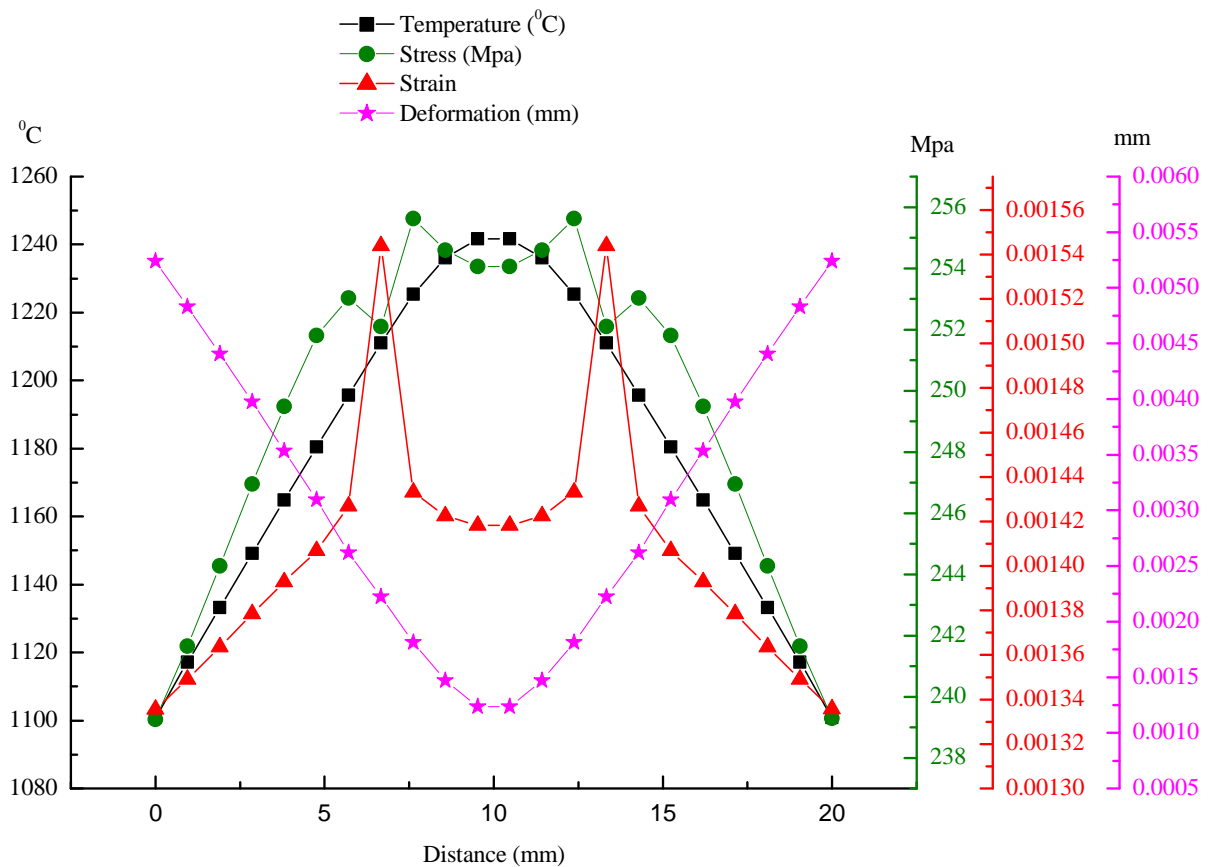


b) Temperature, stress, strain and deformation at profile 1-2

Fig.7. Similar materials, Case 2: STS304+STS304

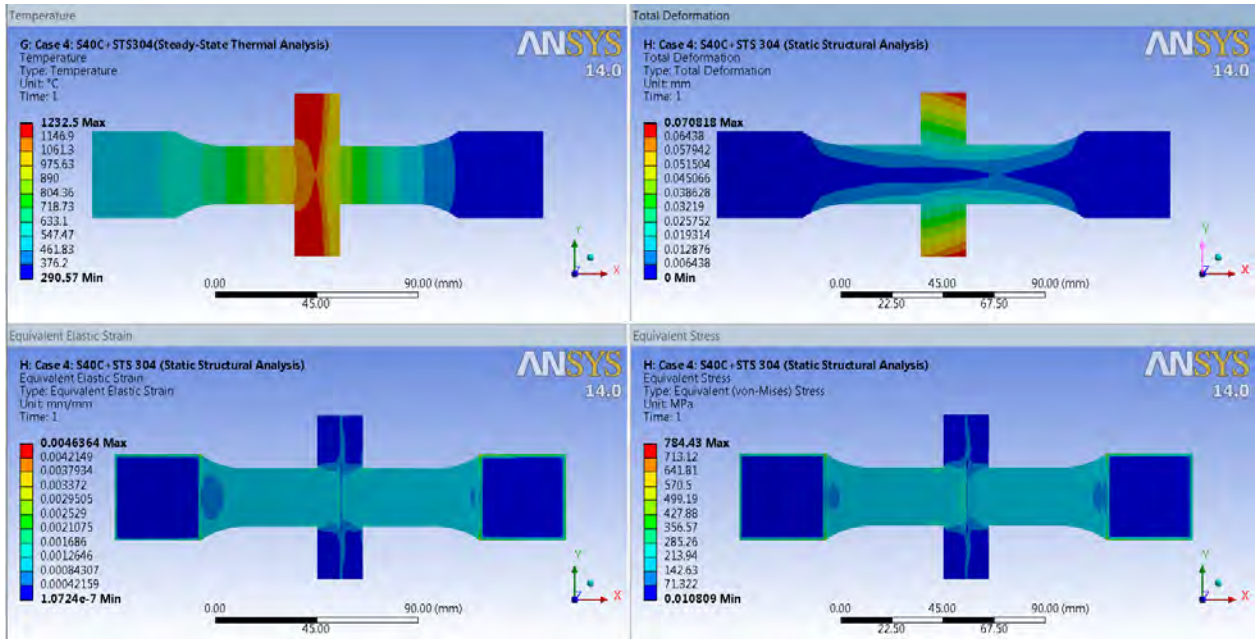


a) Simulation results of temperature, stress, strain and deformation

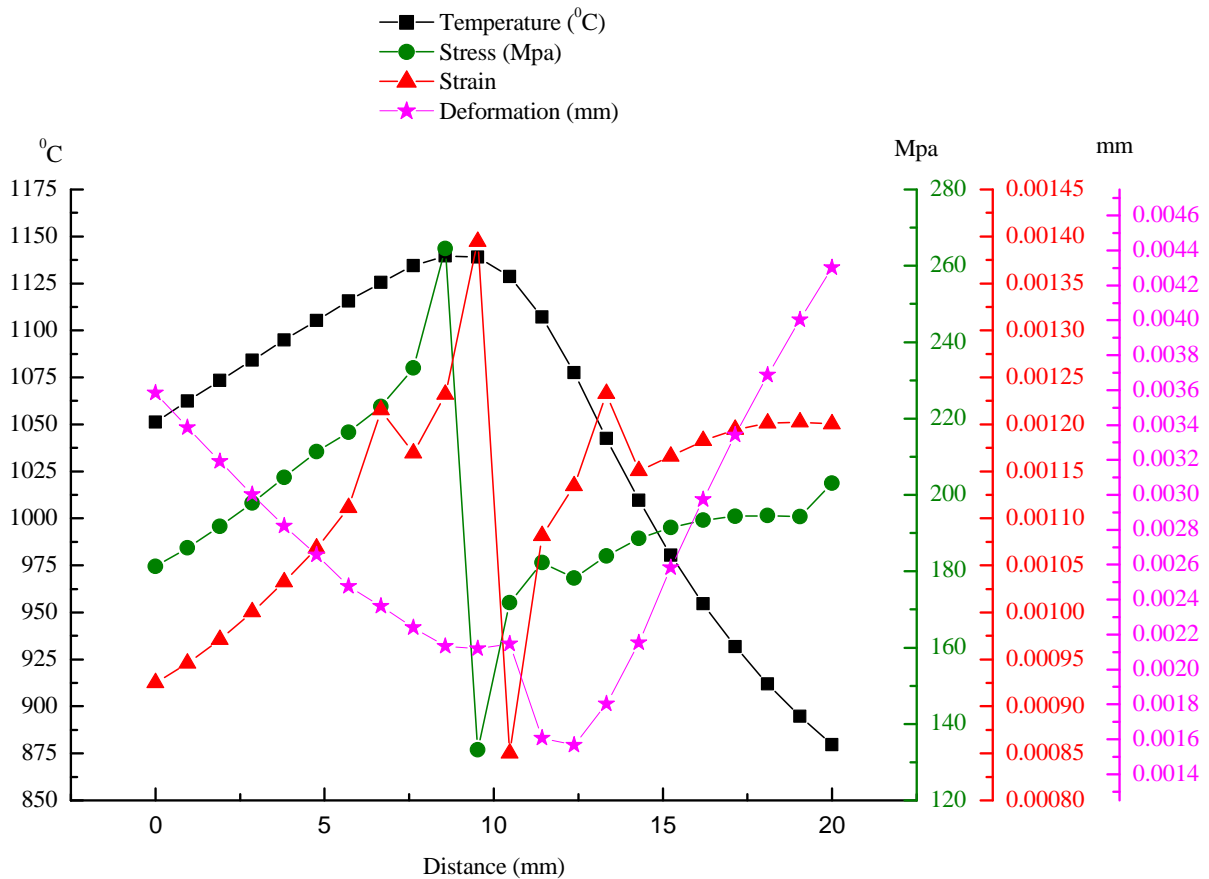


b) Temperature, stress, strain and deformation at profile 1-2

Fig.8. Similar materials, Case 3: STS316+STS316L

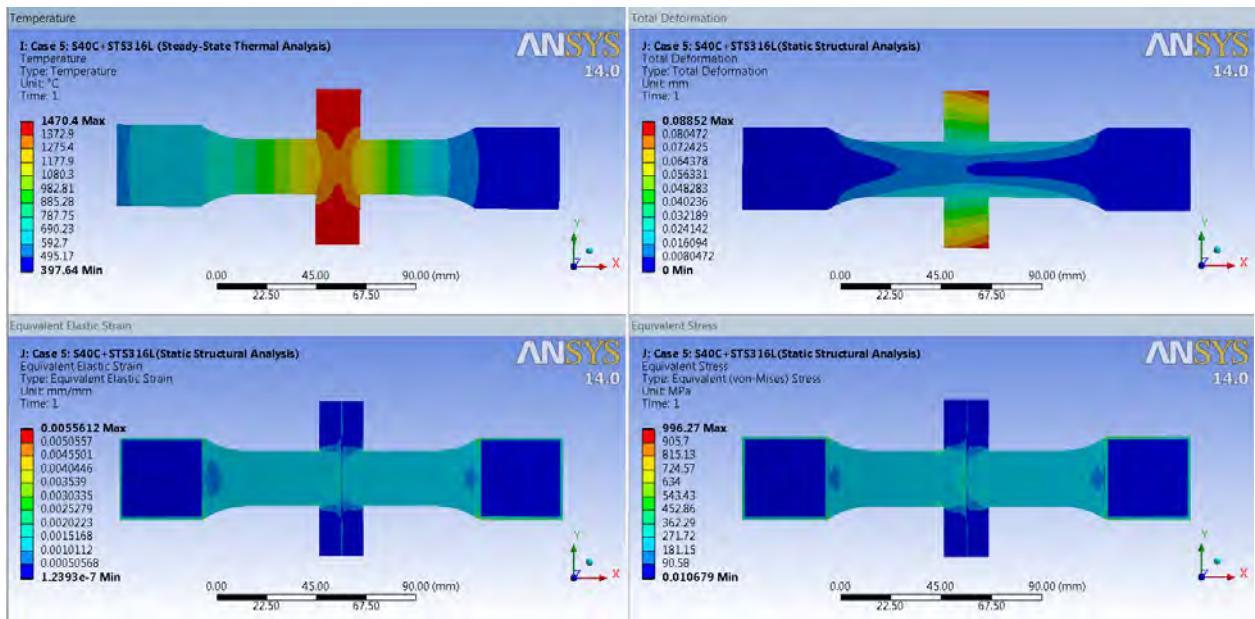


a) Simulation results of temperature, stress, strain and deformation

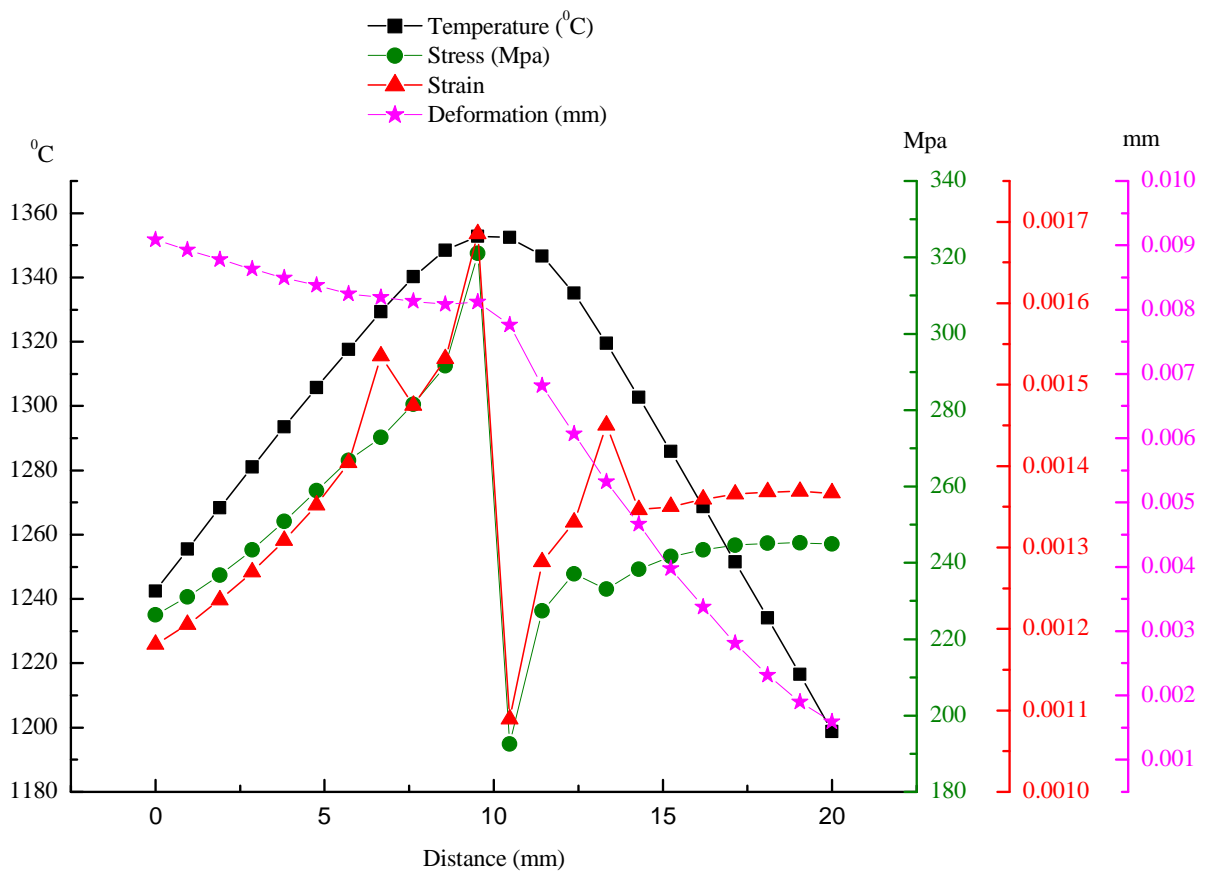


b) Temperature, stress, strain and deformation at profile 1-2

Fig.9. Dissimilar materials, Case 4:S40C+STS304

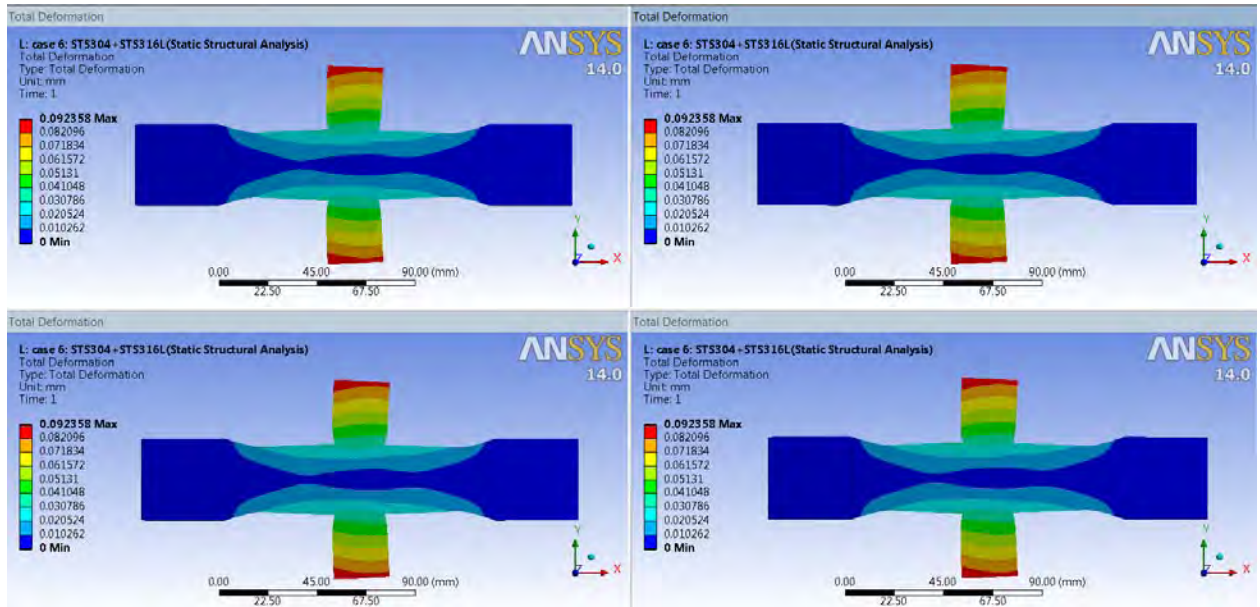


a)
b) Simulation results of temperature, stress, strain and deformation
c)

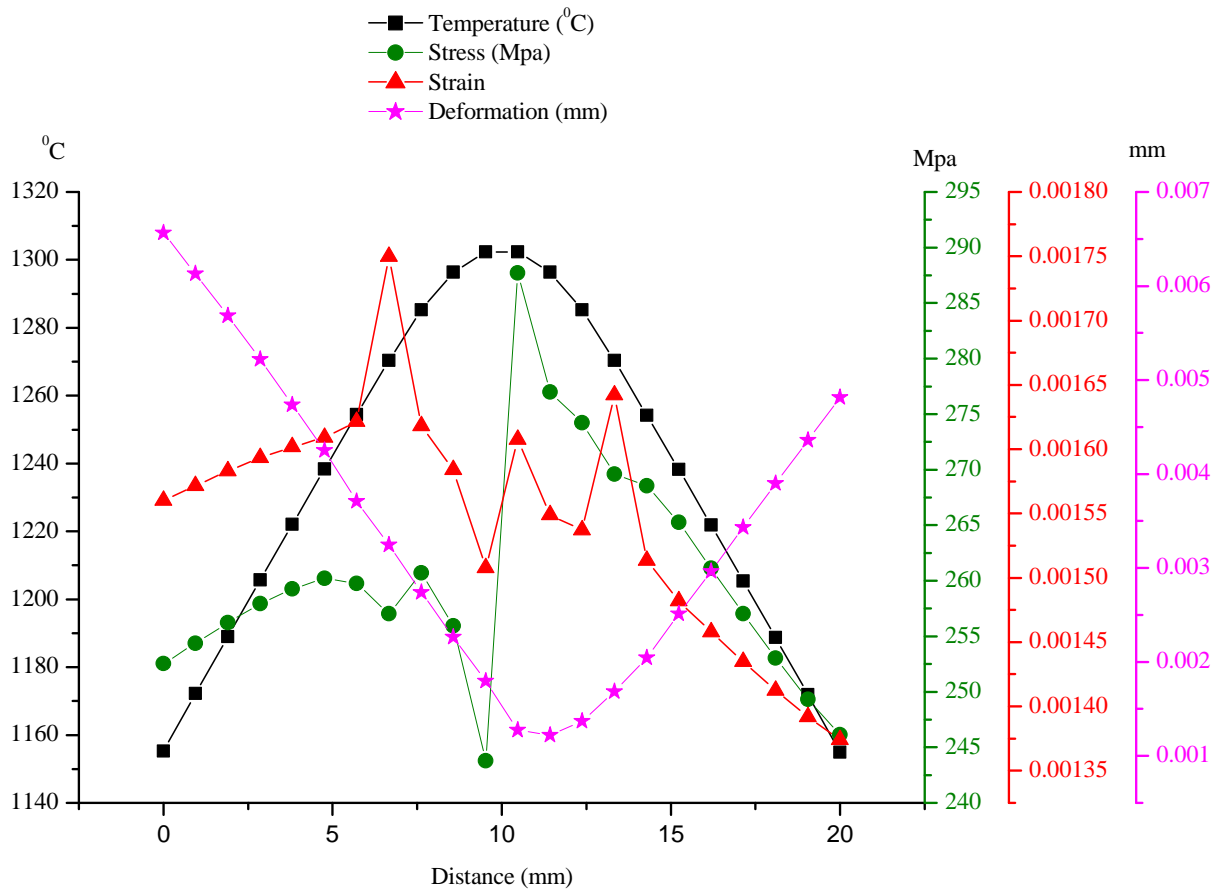


d) Temperature, stress, strain and deformation at profile 1-2

Fig.10. Dissimilar materials, Case 5: S40C+STS316L



a) Simulation results of temperature, stress, strain and deformation



b) Temperature, stress, strain and deformation at profile 1-2

Fig.11. Dissimilar materials, Case 6: STS304+STS316L

For the comparison of temperature, stress, strain and deformation in different six cases (S40C+S40C, STS304+STS304, STS316L+STS316L, S40C+STS304, S40C+STS316L and STS340+STS316L), the temperature, stress, strain and deformation were plotted along the profile 1-2 (90, 0, 0) & (110, 0, 0) as shown in fig.12,13,14 and 15.

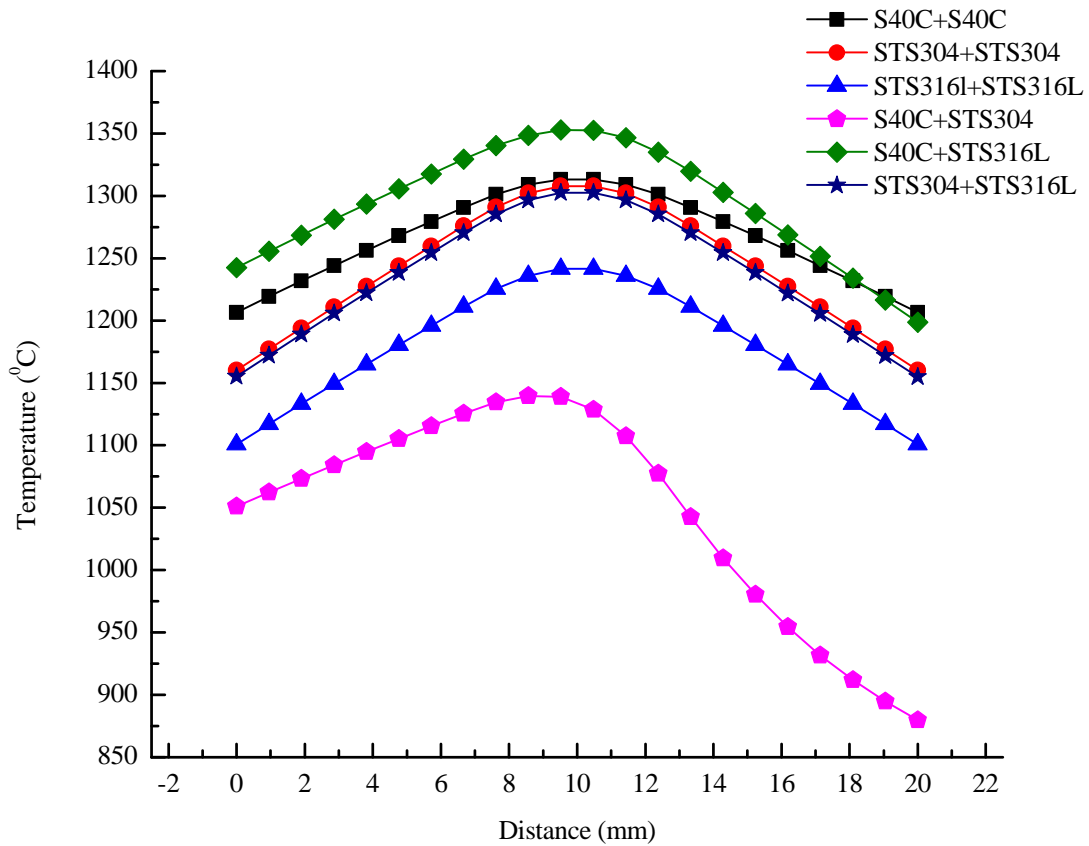


Fig.12. Comparison of temperature along the profile 1-2 for the six different cases.

From the fig.12, it is found that, there is almost similarity in temperature distribution pattern in similar welding materials of case S40C+S40C, STS304+STS304 and STS316L+STS316L but difference in magnitude was observed. Since both the materials A and B are same for the cases S40C+S40C, STS304+STS304 and STS316L+STS316L, the temperature distribution profile seems symmetric from the center line of the specimen. Similarly, it was found that, there is almost similarity in temperature distribution pattern in dissimilar welding material of case S40C+STS316L and STS304+STS316L but huge difference was observed in S40C+STS304. Since the S40C+STS316L, S40C+STS316L and STS304+STS316L are the case of dissimilar materials huge difference in magnitude of temperature was observed as compare to Material A and Material B. The maximum temperature was found in case S40C+STS316L and minimum in case of S40C+STS304.

From fig.13, it is found that, there is almost similarity in stress distribution pattern of similar welding materials of case S40C+S40C, STS304+STS304 and STS316L+STS316L but difference in magnitude was observed. Similarly, it was found that, there is almost similarity in stress distribution pattern of dissimilar welding materials of case S40C+STS304 and S40C+STS316L but huge difference was observed in STS304+STS316L. Comparing the similar and dissimilar materials welding, massive difference in magnitude and pattern was found in stress distribution. It is also found that, the maximum stress was found in case S40C+STS316L and minimum in case S40C+STS304.

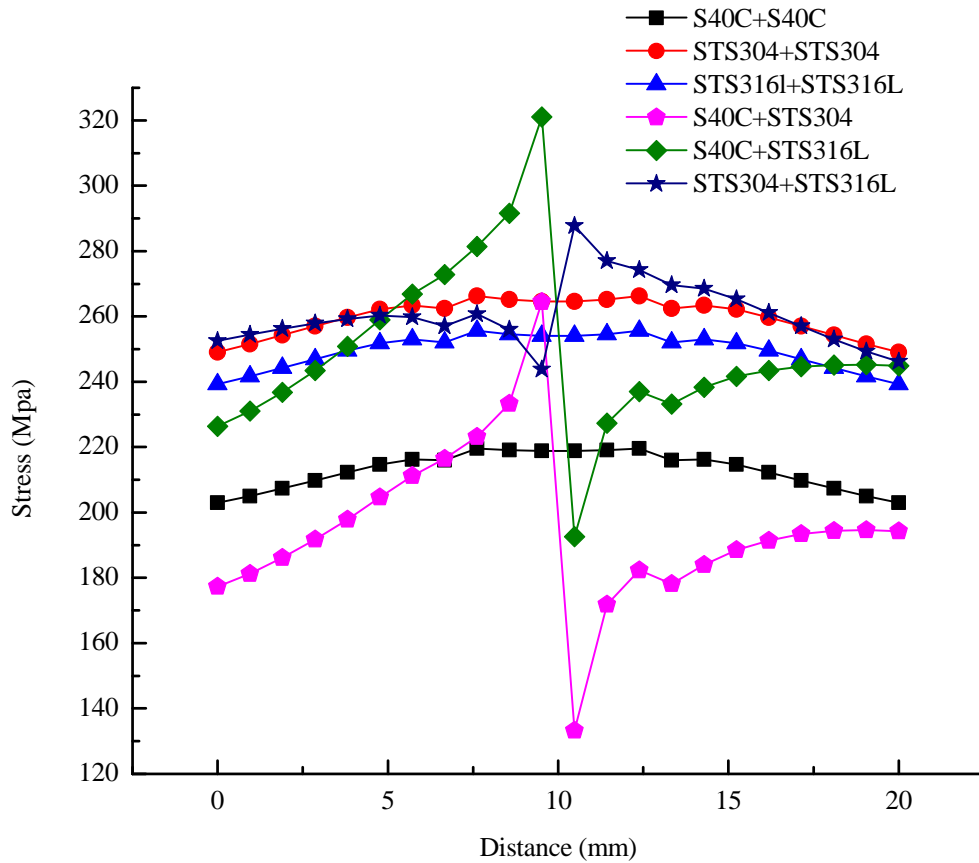


Fig.13. Comparison of stress along the profile 1-2 for the six different cases.

From fig.14, it is found that, there is almost similarity in strain distribution pattern of similar welding materials of case S40C+S40C, STS304+STS304 and STS316L+STS316L but difference in magnitude was observed. Similarly, it was found that, there is almost similarity in strain distribution pattern of dissimilar welding materials of case S40C+STS304 and S40C+STS316L but difference in magnitude was observed. It was also found that, the strain distribution pattern in case STS340+STS316L for dissimilar materials seems different from the other dissimilar materials cases. Comparing the similar and dissimilar materials welding, massive difference in magnitude and pattern was found strain distribution. It is also found that, the maximum strain was found in case STS304+STS304 and minimum in case S40C+STS304.

From fig.15, it is found that, there is almost similarity in deformation in similar welding materials of case S40C+S40C, STS304+STS304 and STS316L+STS316L but difference in magnitude was observed. But deformation of dissimilar welding materials of case S40C+STS304, S40C+STS316L and STS340+STS316L differ to each other's both in profile and magnitude. Comparing the similar and dissimilar materials welding, massive difference in magnitude and pattern in deformation was found. It is also found that, the maximum deformation was found in case S40C+STS316L and minimum in S40C+S40C.

The Table III shows the summary of maximum temperature, stress, strain and deformation along the profile 1-2 in all the six cases.

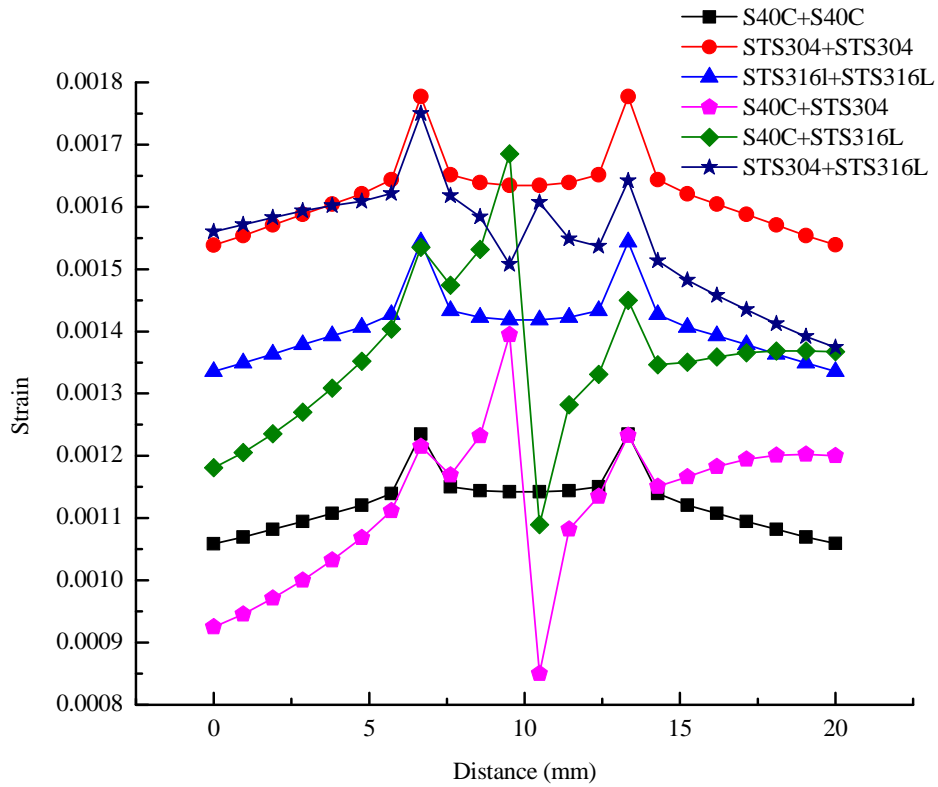


Fig.14. Comparison of strain along the profile 1-2 for all the cases

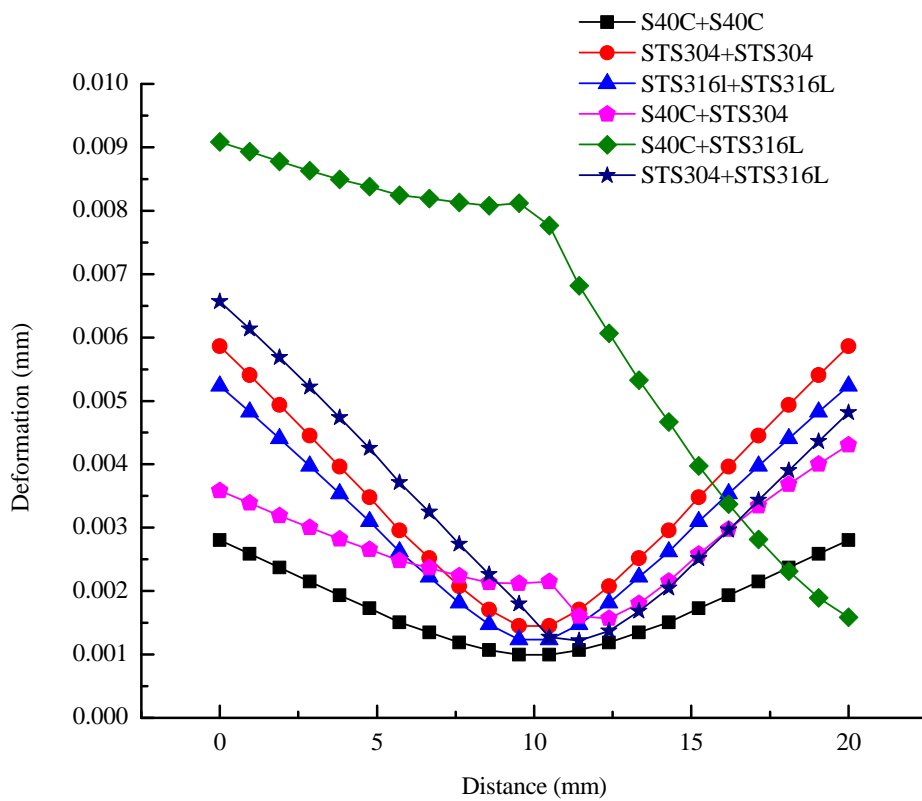


Fig.15. Comparison of deformation along the profile 1-2 for all the cases

TABLE III Summary of maximum and minimum temperature, stress, strain and deformation in all cases

Cases	Material A	Material B	Temperature (°C)		Deformation (mm)		Strain		Stress (MPa)	
			Min	Max	Min	Max	Min	Max	Min	Max
1	S40C	S40C	1260.5	1313.1	0.0009	0.0028	0.0010	0.0012	202.99	219.57
2	STS 304	STS 304	1160.2	1307.9	0.0014	0.0058	0.0015	0.0017	249.05	266.23
3	STS316L	STS316L	1100.9	1241.6	0.0012	0.0052	0.0013	0.0015	239.26	255.62
4	S40C	STS 304	879.62	1139.6	0.0015	0.0043	0.0008	0.0013	133.27	264.46
5	S40C	STS316L	1198.7	1352.8	0.0015	0.0090	0.0010	0.0016	192.58	321.08
6	STS304	STS316L	1154.9	1302.3	0.0012	0.0065	0.0013	0.0017	243.78	287.72

IV. CONCLUSIONS

In this study, 3 Dimensional welding simulation was carried out in the FE software ANSYS in order to predict temperature, stress, strain and deformation in the joining of similar and dissimilar materials. According to the simulated results, some important findings are:

- 1) High temperature gradient exist at the weld zone, where melting occurs by arc heating.
- 2) Higher stress and strain concentrations are located at the weld zone and surrounding heat affected zone.
- 3) The deformation was found maximum in the end of transverse direction and minimum in the end of longitudinal direction as they are simply supported in both ends.
- 4) Being the dissimilar materials, the case STS304+STS316L has the same temperature distribution pattern, deformation, strain and stress profile with as the case of similar materials S40C+S40C, STS304+STS304 and STS316L+STS316L.

ACKNOWLEDGEMENTS

This work were supported by the Basic Science Research Program through the National Research Foundation of Korea (NRF) funded by the Ministry of Education, Science and Technology (No 2010-0023353), and by the Radiation Technology Development Program of the National Research Foundation of Korea (NRF) funded by the Ministry of Science, ICT & Future Planning (No 2014M2A2A9045086).

REFERENCES

- [1] Dean Deng and Hidekazu Murakawa, "Numerical simulation of temperature field and residual stress in multi-pass welds in stainless steel pipe and comparison with experimental measurements," Computational Materials Science, vol. 37, pp. 269-277, 2006
- [2] Zhu XK and Chao YJ, "Effects of temperature-dependent material properties on welding simulation," Computers and Structures, vol. 80, pp. 967-976, 2002
- [3] Vijaykumar N Chalwa, "Welding process simulation using finite element analysis," International Journal of Mechanical Engineering and Computer Applications, vol. 1, pp. 42-47, 2013
- [4] Dragi Stamenkovic and Ivana Vasovic, "Finite Element Analysis of Residual Stress in Butt Welding Two Similar Plates," Scientific Technical Review, vol. LIX, pp. 57-60, 2009
- [5] Mato Peric, Zdenko Tonkovic, Alan Rodic, Martin Surjak, Ivica Garasic, Ivanka Boras and Srecko Svaic, "Numerical analysis and experimental investigation of welding residual stresses and distortions in a T-joint fillet weld," Materials and Design, vol. 53, pp. 1052-1063, 2014
- [6] Nur Syahroni and Mas Irfan Purbawanto Hidayat, "3D Finite Element Simulation of T-Joint Fillet Weld: Effect of Various Welding Sequences on the Residual Stresses and Distortions," Numerical Simulation-From Theory to Industry, 2012, [http://dx. doi. org/10.5772/50192](http://dx.doi.org/10.5772/50192)
- [7] Harshal K Chavan, Gunwant D Shelake and MS kadam, "Effect of heat input and speed of welding on distortion in MIG welding," IJIERD, vol. 3, pp. 42-50, 2012
- [8] Yuan HX, Wang YQ, Shi YJ and Gardner L., "Residual stress distributions in welded stainless steel section," Thin-Walled Structures, vol. 79, pp. 38-51, 2014
- [9] Shu Xu, "Thermal stress analysis of dissimilar welding joints by finite element method," Procedia Engineering, vol. 15, pp. 3860 - 3864, 2011
- [10] Fanrong Kong, Junjie Ma and Radovan Kovacevic, "Numerical and experimental study of thermally induced residual stress in the hybrid laser-GNA welding process," Journal of Materials Processing Technology, vol. 211, pp. 1102-1111, 2011
- [11] Hee Seon Nabg, Han Sur Bang, You Chul Kim, Sung Min Joo, Soon Won Joa and Chang Seung Ro, "Influence of welding stress on the mechanical behavior of externally loaded dissimilar SS400-ST304 steel weldment," Journal of KWJS, vol. 27, pp. 504-511, 2009
- [12] Andrea Capriccioli and Paolo Frosi, "Multipurpose ANSYS FE procedure for welding process simulation," Fusion Engineering and Design, pp. 4863 (8), 2009

AUTHOR INFORMATION

Ranjit Shrestha received his Bachelor degree in Mechanical Engineering from Kathmandu University, Nepal in 2008. He is currently a graduate student of Mechanical Engineering at Kongju National University, Cheonan, Korea. His main research interests include Non-destructive Testing, Infrared Thermography, Machine Vision, Image Processing, Fault Diagnosis, Modeling & Simulation and Renewable Energy Technologies.

Wontae Kim received his Bachelor and Master degrees in Mechanical Engineering from Hanyang University, Korea in 1981 and 1985 respectively. He completed his Ph.D degree in Mechanical Engineering from University of Utah, U.S.A. in 1991. He is currently a Professor at Division of Mechanical & Automotive Engineering, Kongju National University, Cheonan, Korea. His research interests are focused in Non-destructive Testing, Infra-Red Thermography, Energy Saving, Heat Transfer and Fluid Mechanic.

Heesang Park works as a Senior Researcher at Technology Development Team, Korea Research Institute of Smart Material and Structures System Association (KRISMAS), Daejeon, Korea

Jeonghak Park is works as a Senior Researcher at, Safety measurement Center, Korea Research Institute of Standards and Science (KRISS), Daejoen, Korea